Resonance and impact of the 2009 Samoa tsunami around Tutuila, American Samoa

Volker Roeber,[1] Yoshiki Yamazaki,[1] and Kwok Fai Cheung[1]

Received 21 June 2010; revised 30 August 2010; accepted 1 September 2010; published 10 November 2010.

[1] The 2009 Samoa tsunami resulted in severe damage and inundation at Tutuila, American Samoa. The disparity of the impact and the varying accounts of the tsunami along the coast remain one of the most intriguing aspects of the event. We utilize a dispersive wave model to reconstruct the tsunami from the earthquake source for understanding of the wave dynamics around Tutuila. After validation with water-level measurements, a Fast Fourier Transform of the computed surface elevation reveals coupled resonance oscillations between 3 and 18 min period over the insular slope and shelf as well as the fringing reefs. The resonance, which focuses energy according to shelf and embayment configurations, provides an explanation of the runup data and eyewitness accounts and identifies the coastal communities prone to tsunami hazards. **Citation:** Roeber, V., Y. Yamazaki, and K. F. Cheung (2010), Resonance and impact of the 2009 Samoa tsunami around Tutuila, American Samoa, *Geophys. Res. Lett.*, *37*, L21604, doi:10.1029/2010GL044419.

1. Background

[2] An Mw 8.1 earthquake occurred along the Tonga-Kermadec Trench near 172.07°W 15.56°S on September 29, 2009 at 6:48 AM local time (17:48 UTC). Figure 1 shows the locations of water-level stations in the region and the rupture determined by USGS through seismic data inversion. The finite fault solution provides the earthquake rupture in terms of the depth and slip of 420 subfaults over a 210 km by 72 km region on the outer rise of the subducting Pacific Plate. The normal fault rupture generated a tsunami toward Tonga and Samoa. The tsunami arrived in 15 min at Tutuila, American Samoa 200 km from the epicenter and caused 32 casualties and extensive damage to coastal communities. The tide gauge at Pago Pago Harbor registered a maximum surface elevation of 2.2 m, while *Okal et al.* [2010] reported over 10 m of runup at several locations around Tutuila. The DART buoys to the north and south of the main energy beam also recorded clear signals of the tsunami.

[3] We conducted a field survey at Tutuila during November 20–22, 2009 to examine the relation between the physical nearshore environment and the tsunami impact. The rugged, volcanic island sits on a shallow shelf of less than 100 m depth covered by mesophotic corals [*Bare et al.*, 2010]. The insular slope is steep with gradients up to 1:2 on the west side and drops off abruptly to over 3000 m depth in the surrounding ocean. Communities are typically located on narrow coastal plains in embayments sheltered by fringing reefs with steep flanks. The survey found large disparities of impact along the coast. Residents at different communities observed tsunami waves over a wide range of periods and provided varying accounts of the wave height and direction. The common observation of the second or third wave being the largest is contradictory to tsunamis in the near field, where the first wave is usually of highest amplitude.

[4] The seemingly discrepant accounts of the tsunami along the coast and the presence of embayments at the insular shelf suggest trapping and resonant amplification of the tsunami waves around Tutuila during the event. *Kowalik et al.* [2008] and *Munger and Cheung* [2008] have reported large-scale resonance over a continental shelf and along an island chain due to tsunamis. A detailed examination of resonance over an insular shelf and slope complex and its relation to tsunami impact is less immediately evident. The recently developed dispersive wave model NEOWAVE of *Yamazaki et al.* [2009, 2010] makes it possible to resolve the pertinent physical processes including tsunami generation due to earthquake rupture, propagation across the ocean as well as transformation over the insular slope, shelf, and fringing reefs through a two-way nested grid system. Spectral analysis of the high-resolution surface elevation data around Tutuila facilitates a systematic investigation of the oscillation patterns and frequency contents to understand the behavior of the tsunami and provide an explanation of the tragedy.

2. Modeling and Validation

[5] The planar fault model of *Okada* [1985] provides the seafloor deformation from the USGS finite fault solution for modeling of the 2009 Samoa tsunami through NEOWAVE. The staggered finite difference model builds on the nonlinear shallow-water equations with a non-hydrostatic pressure term to account for weakly dispersive waves and a momentum conservation scheme to approximate breaking waves as bores or hydraulic jumps. We utilize four levels of two-way nested grids as shown in Figure 1. The first level includes the rupture zone, the three DART buoys, and the Samoa Islands at 1 arcmin (~2000-m) resolution, while the second and third levels cover Tutuila at increasing resolution of 7.5 (~250 m) and 1.5 (~50 m) arcsec. The fourth level grid at Pago Pago Harbor allows computation of the tide gauge signal at high resolution of 0.3 (~10 m) arcsec. The digital elevation model consists of the NGDC tsunami inundation grid at 10 m resolution, the University of Hawaii SOEST multibeam data and the IKONOS satellite data both at 5 m resolution, and the 0.5-arcmin (~1000-m) GEBCO data for the surrounding ocean.

[6] The computation covers 5 hours of event time with 2-sec output intervals until the tsunami wave activities around Tutuila subside. A Fast Fourier Transform of the computed

[1]Department of Ocean and Resources Engineering, University of Hawaii at Manoa, Honolulu, Hawaii, USA.

0094-8276/10/2010GL044419

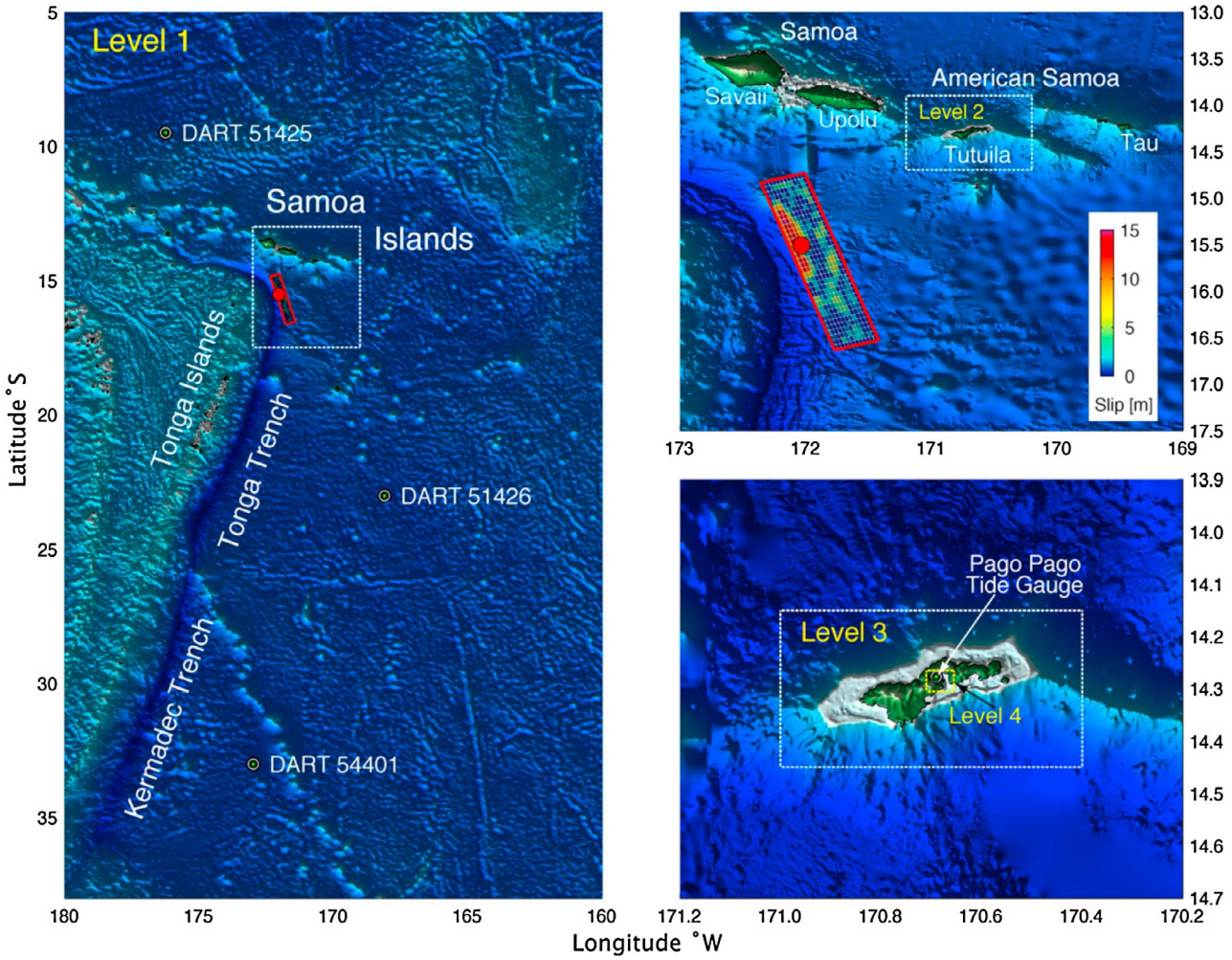

Figure 1. Nested computational grids, rupture configuration, and locations of water-level stations.

surface elevation provides the amplitude $Y(f)$ and phase $\theta(f)$ as functions of frequency f. Figure 2 shows the computed and recorded tsunami time series and spectra at the Pago Pago tide gauge and the three DART buoys in the region. The model reproduces the initial waves at the tide gauge and captures the distinct oscillations at 11 and 18 min, which are indicative of resonance in the harbor. The DART buoys roughly along the strike of the rupture did not record the main tsunami waves propagating toward Tutuila, while DART 51426 and 54401 show reflected waves from Tutuila about 100 and 180 min, respectively, after the earthquake. The discrepancy between the computed and recorded initial waveforms at the DART buoys is likely due to a secondary rupture in the forearc recently reported by *Lay et al.* [2010]. The good agreement at the Pago Pago tide gauge and the reproduction of the reflected waves at DART 51426 and 54401 validate the primary source mechanism and the resulting tsunami for assessment of the impact at Tutuila.

3. Resonance Modes

[7] Resonance amplification of the 2009 Samoa tsunami occurs at a number of periods between 3 to 18 min associated with standing waves over the insular slope and shelf complex as well as the fringing reefs in embayments around Tutuila. The channels between Tutuila and the neighboring islands are wide and deep to prevent resonance oscillations at the regional scale as seen along the Hawaiian Island chain [*Munger and Cheung*, 2008]. Figure 3 shows the spectral amplitude plots for eight representative oscillation modes to provide insights into the tsunami impact around Tutuila. The 100-m depth contour shows the outline of the insular shelf, while the 3000-m contour indicates the extent of the insular slope. Despite the southwest approach of the tsunami, the energy distribution is rather even over the insular shelf demonstrating the eigen modes of the geomorphology. The phase plots in Figure 4 show some of the oscillation modes contain partial standing waves, which do not have well defined nodes, because of the irregular shelf and coast configurations. Standing waves have the same phase within an antinode and an abrupt 180° phase shift to adjacent antinodes, while partial standing waves show gradual phase variations across the nodes. A uniform phase variation would indicate progressive waves.

[8] The first resonance at 18 min corresponds to the fundamental mode of Pago Pago Harbor. The phase plot shows a system of large-scale partial standing waves on the north

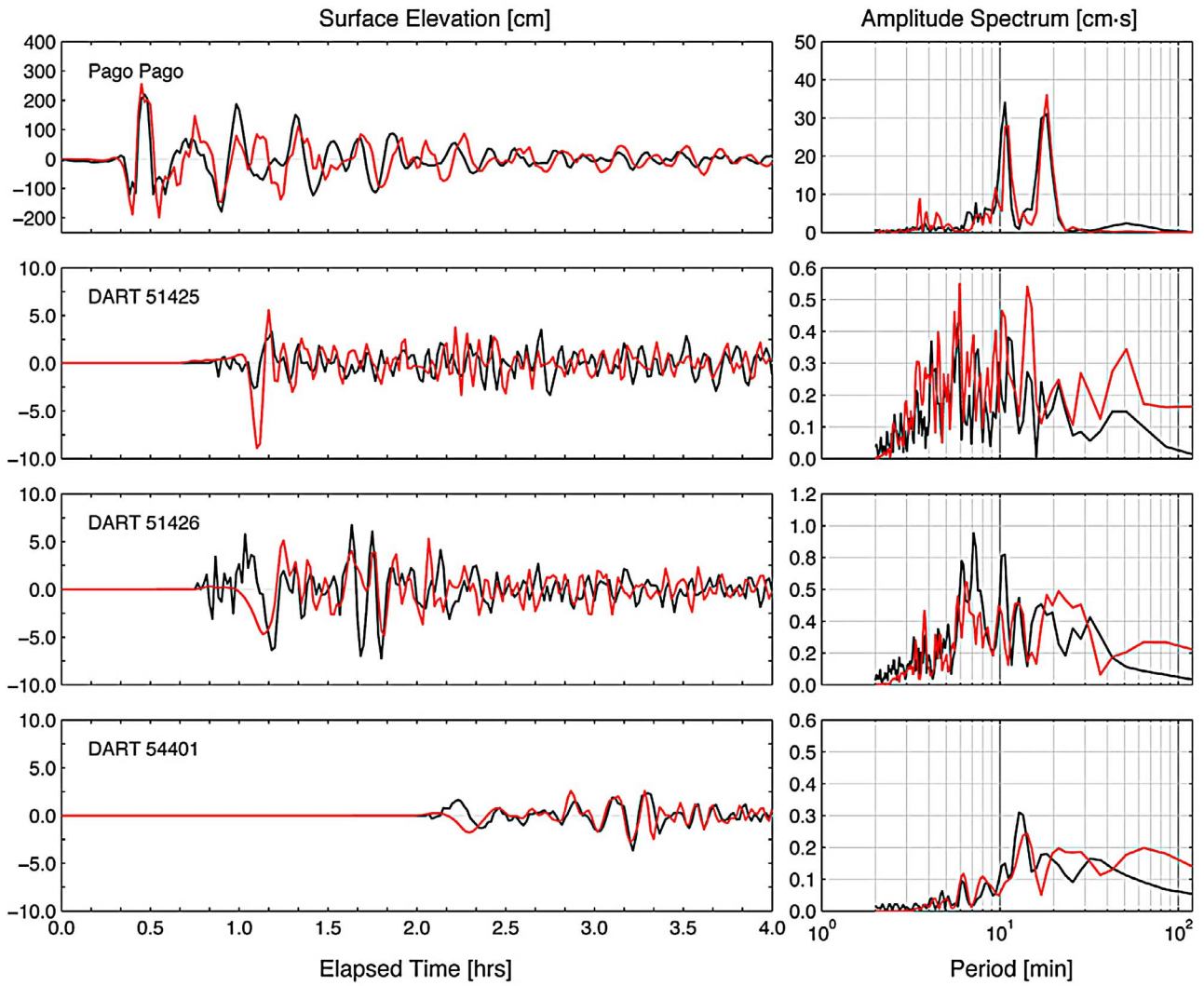

Figure 2. Waveforms and amplitude spectra at water-level stations. Red and black lines denote computed and recorded data, respectively.

and south sides of Tutuila. Most of the partial standing waves have very small amplitude not noticeable in the amplitude plot, but the power can be considerable because of the water depth. The resonance in Pago Pago Harbor and the partial standing waves are coupled with a 180° phase difference resulting in the minor amplification in the embayment outside the harbor. At 13 min, resonance amplification occurs over the insular shelf with well-defined antinodes on the west and east sides of the island. The two antinodes have opposite phases and interact through the partial standing waves over the insular slope. Pago Pago Harbor still oscillates at the fundamental mode with the node shifted inward and at a much lower energy level. At 10 min 56 sec, the resonance oscillation in the harbor extends to the outside embayment with a node at the entrance. An antinode develops at the east end of the insular shelf. The partial standing waves retreat from the shelf and become out-of-phase over the northern and southern insular slope. This large-scale oscillation becomes less coherent between the two sides of the insular slope at the higher resonance modes.

[9] Resonance amplification occurs over the entire insular shelf at 7 min 52 sec. The oscillation resembles the pattern of mode-0 standing edge waves with well-defined nodes and antinodes along the shore and a gradual decline of the amplitude offshore. *Eckart* [1952] provided the shallow-water dispersion relation for mode-n edge waves over a plane beach as

$$c = \frac{gT}{2\pi}(2n+1)s$$

where c is celerity, g is gravitational acceleration, T is period, and s is beach slope. The 1:60 average slope on the shelf gives an estimated length of the mode-0 edge waves at 5.8 km, which is close to the average wavelength of 7 km depicted along the north shore in the amplitude plot. Resonance oscillations begin to develop in embayments along the north shore. The phase plot shows a system of small amplitude, partial standing waves over the western and northern insular slope. The 180° phase difference between the oscillations across the slope, shelf, and embayments indicate coupling of the standing waves at three geographic scales.

[10] The phase plots have been instrumental in deciphering complex oscillation patterns not obvious in the amplitude plots. At 7 min, the system of partial standing waves switches to the southern insular slope and the shelf oscillation mode

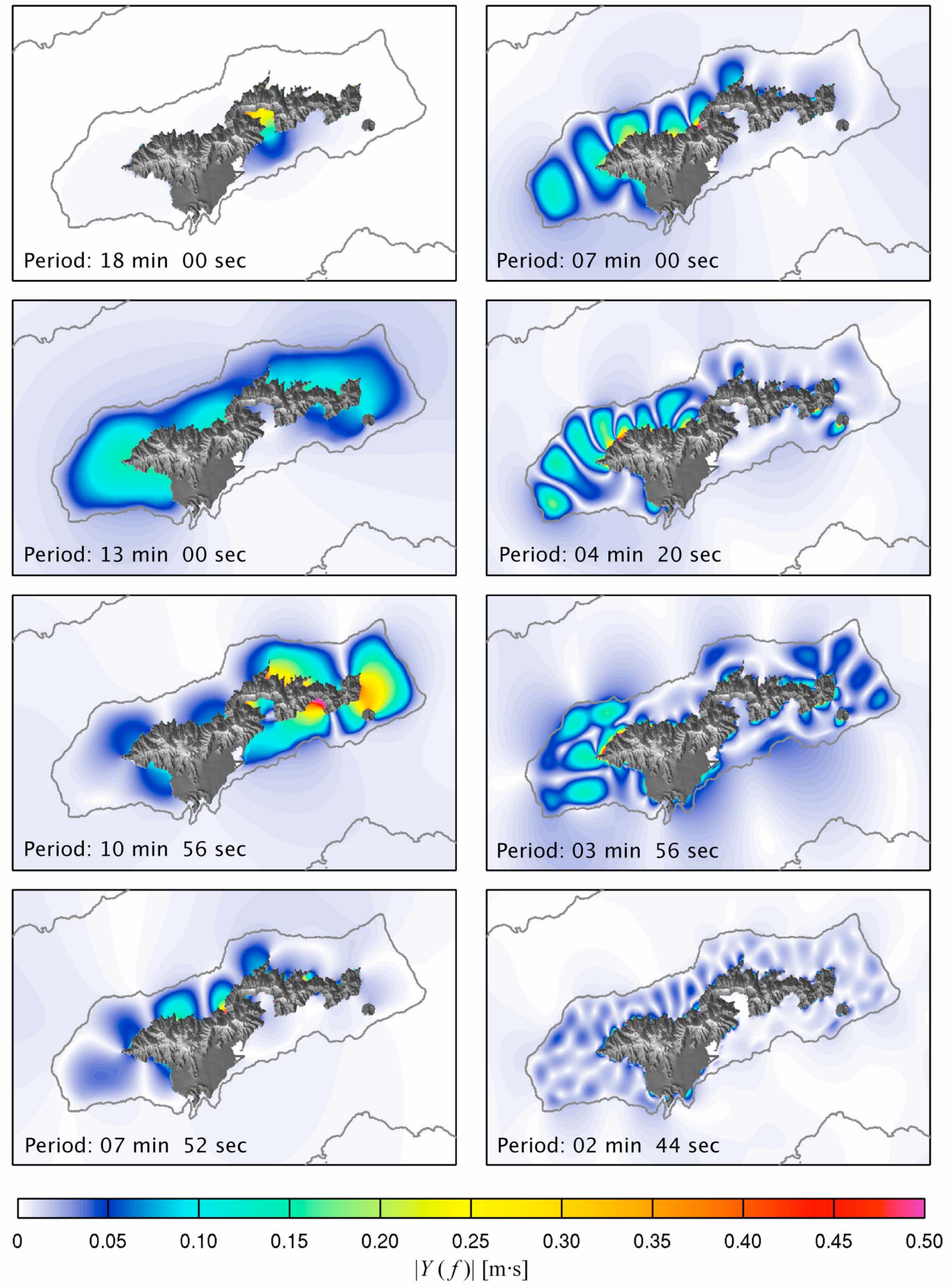

Figure 3. Amplitude of resonance modes around Tutuila. Contour lines indicate 100 m and 3000 m depth.

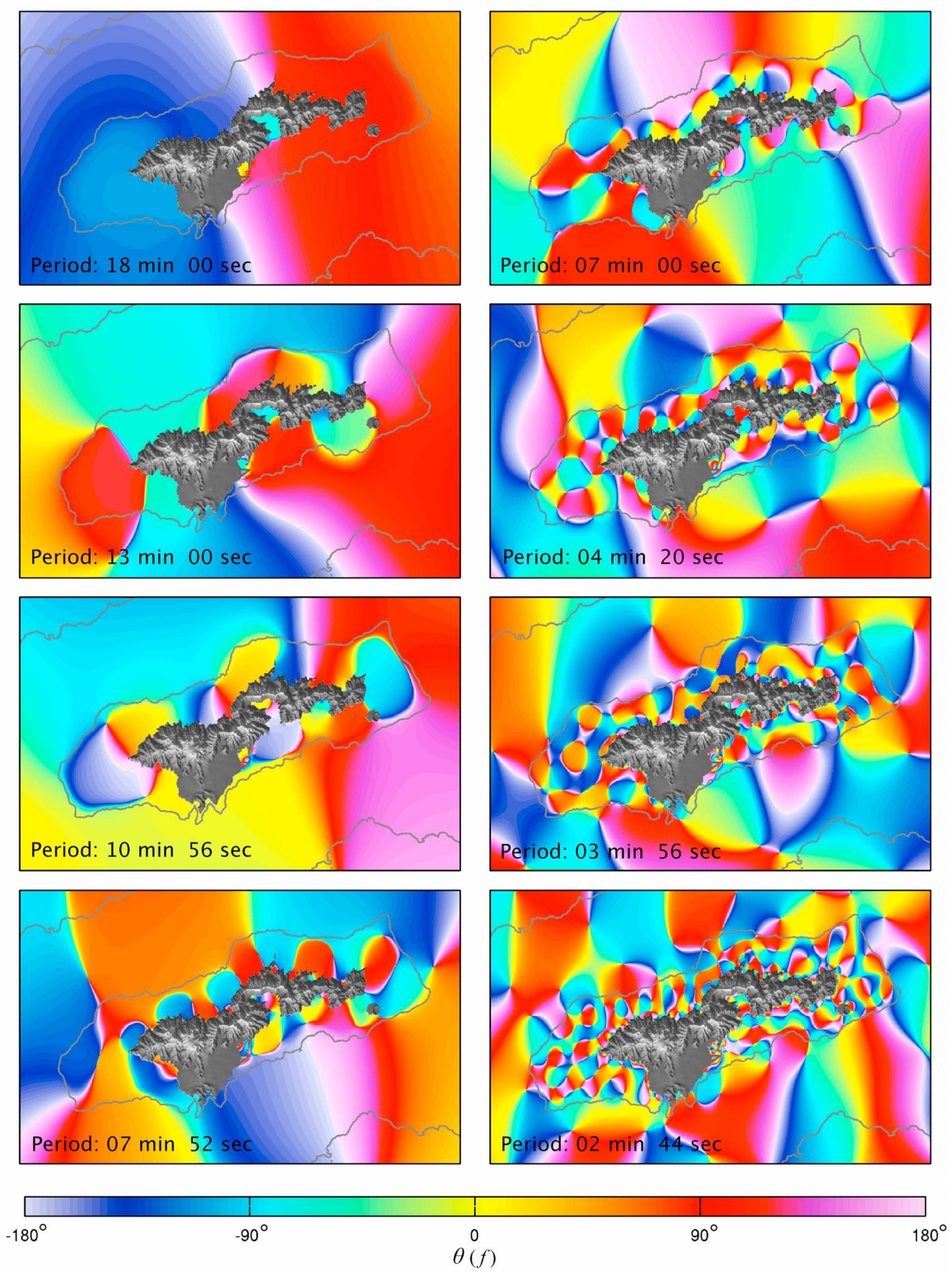

Figure 4. Phase angle of resonance modes around Tutuila. Contour lines indicate 100 m and 3000 m depth.

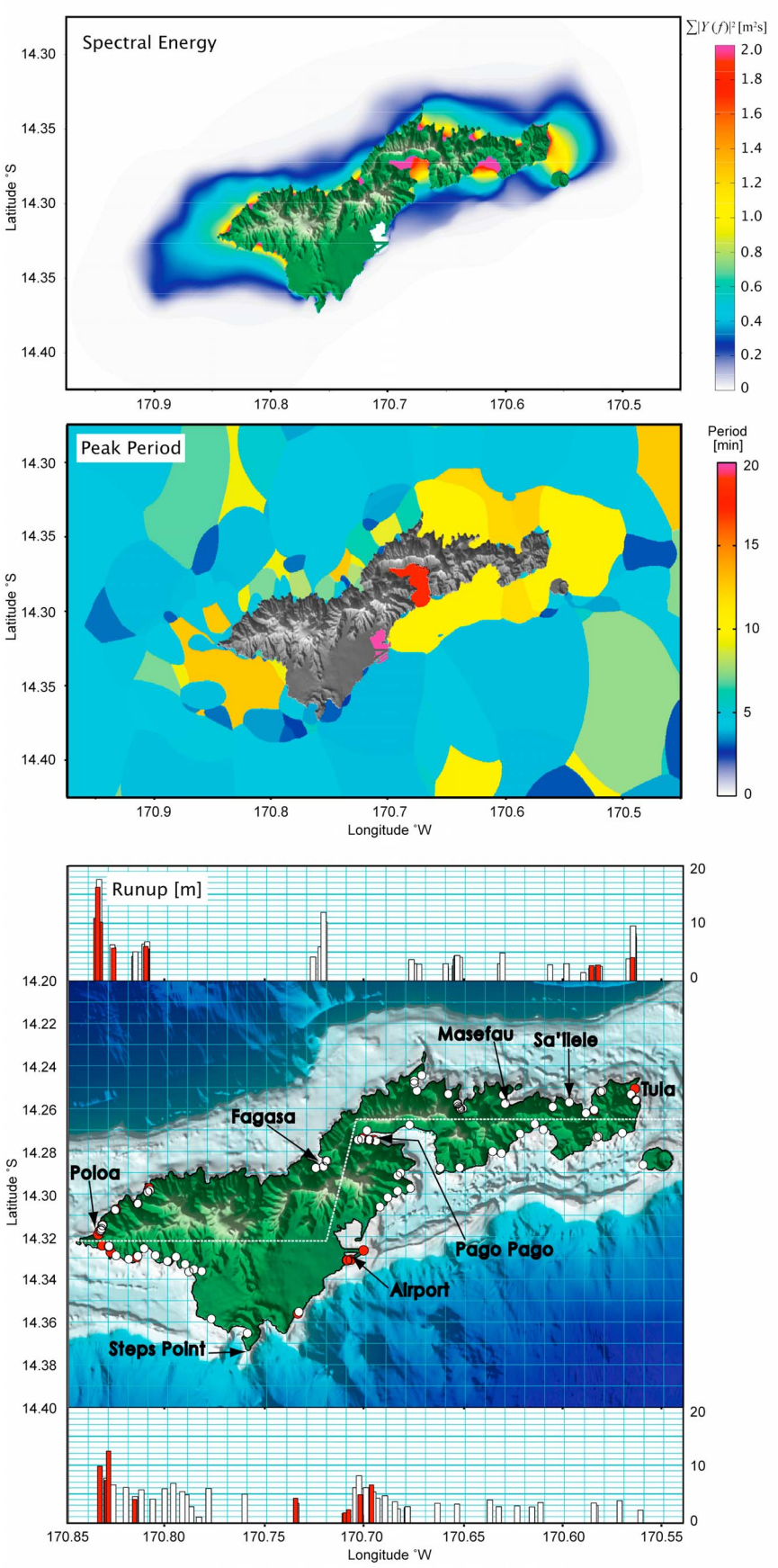

Figure 5. Spectral energy, peak period, and recorded runup around Tutuila. White and red bars indicate runup data from *Okal et al.* [2010] and *Koshimura et al.* [2009], respectively.

has an additional offshore antinode over the wide insular shelf on the west. The 4 min 20 sec resonance mode has two offshore antinodes over the shelf and a system of partial standing waves around the insular slope. Elaborate systems of standing waves begin to form over the shelf and slope with significant amplification in embayments at 3 min and 56 sec. Well-defined standing waves are present in Pago Pago Harbor albeit with low amplitude. The highest detectable resonance mode over the entire shelf occurs at 2 min 44 sec with notable amplification at the fringing reefs.

4. Tsunami Hazard Areas

[11] The resonance modes identify the areas prone to large oscillations and provide an explanation to the tsunami and impact observed along the Tutuila coast. Figure 5 shows the computed spectral energy and peak period together with the runup data from *Koshimura et al.* [2009] and *Okal et al.* [2010]. The resonance energy covers the entire insular shelf, but its level and peak period vary markedly along the coast as reported by eyewitness. The most prominent is Pago Pago, where the long, narrow harbor captures long period waves of up to 18 min. The water depth over the insular shelf is relatively uniform. The east and west sides of Tutuila with wider shelf are susceptible to oscillations with periods over 10 min, whereas the narrower shelf on the north results in a mix of short period oscillations between 4 and 10 min. Fringing reefs and small embayments amplify the nearshore energy and develop local oscillation modes with 2~4 min periods adjacent to the shore. The resonance period influenced the total number of destructive waves being observed during the tsunami event with 4–5 waves reported on the west side and 2–3 waves counted in several villages on the east side. The small-amplitude partial standing waves over the insular slope dissipate slowly and provide a source of energy to sustain the shelf oscillations for several hours.

[12] High concentration of resonance energy generally occurs in the embayments that have large reported runup. The tsunami reached a 17-m elevation at Poloa on the west side and produced runup heights of 12 m at Fagasa, 10 m at Tula, and 8 m at Pago Pago. All of these locations have fringing reefs extending 100 to 200 m from the shores. Contrary to the commonly belief that coral reefs provide protection to coastal communities from tsunamis, the shallow lagoons may trap tsunami energy and exacerbate the impact of short-period dispersive waves. Eyewitness at some of villages provided descriptions of what appear to be turbulent bores over the reefs. *Roeber et al.* [2010] showed fringing reefs with steep flanks transform non-breaking long waves into more dangerous bores.

[13] The narrow, crescent shape embayment at Poloa coincides with antinodes of the resonance modes at 7 min, 4 min 20 sec, and 3 min 56 sec. The amplitude of the oscillation at 3 min 56 sec increases sharply across the nearshore reef system as shown in Figure 3. This local amplification provides an explanation for the large runup even though the energy levels of these short-period resonance modes are moderate. Fagasa is a horseshoe shape bay with a minor constriction in the middle forming a narrower inner basin. The 7 min 52 sec and 7 min resonance modes have antinodes at Fagasa with significant amplification in the inner basin surrounded by reefs. Tula is located on an open coast in front of a 40~50 m deep basin at the east end of the insular shelf. The basin resonates at 10 min 56 sec with the peak energy at the headland immediately south of Tula, where the maximum runup was recorded. Pago Pago Harbor is prone to high-amplitude oscillations because a number of resonance modes can develop in the long, narrow harbor and the outside embayment. The resonance modes at 18 min and 10 min 56 sec have high-amplitude antinodes at the inner harbor causing the large runup through constructive interference at the well-sheltered location from the tsunami.

[14] The shorelines not affected by resonance oscillations correspond well with locations with relatively minor impact. An example is Sa'ilele, which is located near a node of most resonance modes. The village sustained no tsunami inundation or damage despite its beachfront location. The neighboring village Masefau, which was affected by at least one resonance mode, suffered heavy damage to infrastructure and properties. The southern side of Tutuila from Steps Point to the airport experienced only minor runup despite its location in the path of direct energy approach. The steep drop-off of the island shelf limits the oscillation of most resonance modes in front of the coastline. The runup of 4 to 6 m around Steps Point corresponds to local amplification across the reef systems at the 2 min 44 sec resonance.

5. Conclusions

[15] The property damage and casualties at Tutuila during the 2009 Samoa tsunami show strong correlation with the geomorphology of the island. Coupled resonance oscillations occurred over the insular slope, insular shelf, and fringing reefs. The embayments with prominent headlands further amplify the resonance oscillations that resulted in localized impacts and varying accounts of the tsunami waves by eyewitness along the coast. Standing and partial standing waves develop on the north and west sides of the island with periods between 3 to 10 min, while the water over the eastern part of the shelf resonates with 9 to 11 min period. The long and deep harbor basin at Pago Pago has natural periods between 4 and 18 min that coincide with the resonance over the insular slope and shelf.

[16] The 2009 Samoa tsunami serves as a benchmark study of tsunami risks for island communities around the world. Though the western side of the island facing the tsunami source saw the highest runup, severe wave impact and destruction are evident along the eastern and northern shores of the island. The shallow reefs, in some instances, provided little protection to the coastal communities and transformed the tsunami waves into more dangerous conditions. The knowledge on local resonance is of greater importance to hazard mitigation than the origin and direction of the tsunami. Even without detailed information on the tsunami source, implementation of the presented methodology with hypothetical events can provide insights into potential tsunami threats for emergency planning and management.

[17] **Acknowledgments.** This paper is funded in part by a grant/cooperative agreement from the National Oceanic and Atmospheric Administration (NOAA), Project R/IR-2, which is sponsored by the University of Hawaii Sea Grant College Program, School of Ocean and Earth Science and Technology (SOEST), under Institutional grant NA09OAR4170060 from NOAA Office of Sea Grant, Department of Commerce. The NOAA Integrated Ocean Observing System Program provided additional support through grant NA08NOS4730299. The authors would like to thank Goeke and Phil Wiles for their comments on this manuscript, Gavin P. Hayes for

supplying the finite fault solution of the 2009 Samoa Earthquake and Ephraim Temple for providing logistic support during our survey. The views expressed herein are those of the authors and do not necessarily reflect the views of NOAA and any of its sub-agencies. UNIHI-SEAGRANT-JC-09-31. SOEST contribution 7999.

References

Bare, A. Y., K. L. Grimshaw, J. J. Rooney, M. G. Sabater, D. Fenner, and B. Carroll (2010), Mesophotic communities of the insular shelf at Tutuila, American Samoa, *Coral Reefs*, *29*, 369–377, doi:10.1007/s00338-010-0600-y.

Eckart, C. (1952), The propagation of gravity waves from deep to shallow water, *Natl. Bur. Stand. Circ.*, *20*, 165–173.

Koshimura, S., Y. Nishimura, Y. Nakamura, Y. Namegaya, G. J. Fryer, A. Akapo, L. S. Kong, and D. Vargo (2009), Field survey of the 2009 tsunami in American Samoa. *Eos Trans. AGU*, *90*(52), Fall Meet. Suppl., Abstract U23F-07.

Kowalik, Z., J. Horrillo, W. Knight, and T. Logan (2008), Kuril Islands tsunami of November 2006: 1. Impact at Crescent City by distant scattering, *J. Geophys. Res.*, *113*, C01020, doi:10.1029/2007JC004402.

Lay, T., C. J. Ammon, H. Kanamori, L. Rivera, K. Koper, and A. Hutko (2010), The 2009 Samoa-Tonga great earthquake triggered doublet, *Nature*, *466*(7309), 964–968, doi:10.1038/nature09214.

Munger, S., and K. F. Cheung (2008), Resonance in Hawaii waters from the 2006 Kuril Islands tsunami, *Geophys. Res. Lett.*, *35*, L07605, doi:10.1029/2007GL032843.

Okada, Y. (1985), Surface deformation due to shear and tensile faults in a half space, *Bull. Seismol. Soc. Am.*, *75*(4), 1135–1154.

Okal, E. A., et al. (2010), Filed survey of the Samoa tsunami on 29 September 2009, *Seismol. Res. Lett.*, *81*(4), 577–591, doi:10.1785/gssrl.81.4.577.

Roeber, V., K. F. Cheung, and M. H. Kobayashi (2010), Shock-capturing Boussinesq-type model for nearshore wave processes, *Coastal Eng.*, *57*(4), 407–423, doi:10.1016/j.coastaleng.2009.11.007.

Yamazaki, Y., Z. Kowalik, and K. F. Cheung (2009), Depth-integrated, non-hydrostatic model for wave breaking and runup, *Int. J. Numer. Methods Fluids*, *61*(5), 473–497, doi:10.1002/fld.1952.

Yamazaki, Y., K. F. Cheung, and Z. Kowalik (2010), Depth-integrated, non-hydrostatic model with grid nesting for tsunami generation, propagation, and run-up, *Int. J. Numer. Methods Fluids*, doi:10.1002/fld.2485, in press.

K. F. Cheung, V. Roeber, and Y. Yamazaki, Department of Ocean and Resources Engineering, University of Hawaii at Manoa, Holmes Hall 402, 2540 Dole St., Honolulu, HI 96822, USA. (cheung@hawaii.edu)